THEORY AND APPLICATIONS OF TRANSPORT IN POROUS MEDIA

Emerging Topics in Heat and Mass Transfer in Porous Media

From Bioengineering and Microelectronics to Nanotechnology

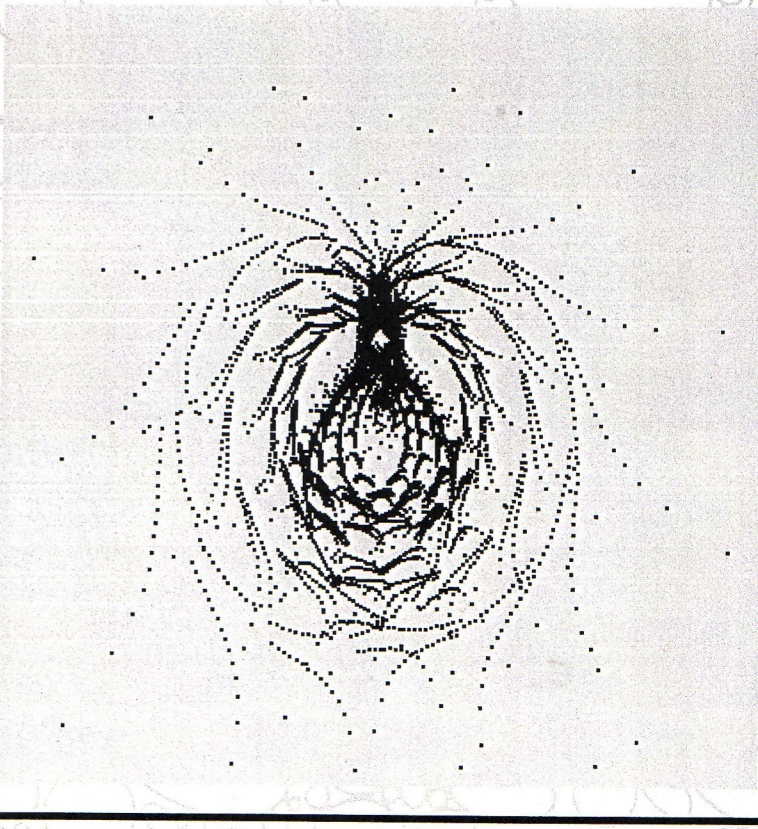

Peter Vadász (Ed.)

Macromolecular Transport in Arterial Walls: Current and Future Directions

K. Khanafer and K. Vafai

Abstract Relevant mathematical models associated with the transport of macromolecules in the blood stream and in the arterial walls are reviewed in this work. A robust four-layer model (endothelium, intima, internal elastic lamina and media) based on porous media concept and accounting for selective permeability of each porous layer to certain solutes is presented to describe the transport of macromolecules in the arterial wall coupled with the transport in the lumen. The variances in the current models are analyzed and discussed. Future direction in developing a rigorous mathematical model for transport in arterial walls using porous media theory and fluid-structure interaction approach is outlined in this study.

1 Introduction

Atherosclerosis, which comes from the Greek words athero (meaning gruel or paste) and sclerosis (hardness), is a form of vascular disease that is commonly located in the large- and medium-size arteries. Atherosclerosis is a slow, progressive disease that may start in childhood. It can affect the arteries of the brain, heart, kidneys, and the arms and legs. It is caused by the slow buildup of fatty substances, cholesterol, cellular waste products, calcium and other substances found in the blood within the arterial walls. This buildup is called plaque. It has been suggested that the transport of the low-density lipoprotein (LDL) from the blood into the arterial wall and its accumulation within the wall play an important role in the process of atherogenesis (Ross 1993, Hoff et al. 1975, Schwenke et al. 1993, Newby and Zaltsman 2000). This transport process is termed "arterial mass transport" and is influenced by blood flow in the lumen and transmural flow in the arterial wall.

Several mathematical models have been developed to model the transport of macromolecules, such as low density lipoproteins (LDLs), from the arterial lumen to the

K. Khanafer
University of Michigan, Ann Arbor, MI, USA

K. Vafai
University of California, Riverside, CA, USA
e-mail: vafai@engr.ucr.edu

P. Vadász (ed.), *Emerging Topics in Heat and Mass Transfer in Porous Media*,

arterial walls and their accumulation in the wall (Fry 1985, Huang and Tarbell 1997, Stangeby and Ethier 2002a,b, Karner et al. 2001, Karner and Perktold 2000, Ai and Vafai 2006, Yang and Vafai 2006). Prosi et al. (2005) have classified these models in three major categories. The simplest model is referred to as wall-free model in which the arterial wall is described by simplified boundary conditions (Back et al. 1977, Ehrlich and Friedman 1977, Rappitsch and Perktold 1996, Ethier 2002, Wada and Karino 1999, 2000, 2002, Qui and Tarbell 2000). This model has been used to investigate oxygen and LDL transport in idealized and physiological arterial models. This model has the advantage of being computationally expedient and provides qualitative information on mass transfer in the blood lumen. However, the main drawback of this model is its limitation in computing concentration profiles within the arterial wall. A more realistic approach is named lumen-wall models which approximate the complex structure of the arterial wall by a simple homogeneous layer. Such models, originally proposed by Moore and Ethier (1997), have been used to study the mass transport of LDL within the arterial wall by Stangeby and Ethier (2002a,b). They used a model that coupled transmural fluid flow to the motion of the flowing blood in the arterial lumen. The most realistic models are multilayer models, which break the arterial wall down into several layers, precisely the endothelium, intima, internal elastic lamina and media, and model the transport within the wall, either at the microscopic (Yuan et al. 1991, Huang et al. 1994, Huang and Tarbell 1997, Tada and Tarbell 2004) or macroscopic (Fry 1985, 1987, Karner et al. 2001, Prosi et al. 2005, Ai and Vafai 2006, Yang and Vafai 2006) levels. The multilayer model was found to provide the most realistic information on the dynamics of chemicals (especially macromolecules) within the wall.

2 Mathematical Models

2.1 Wall-Free Model

Rappitsch and Perktold (1996) and Rappitsch et al. (1997) presented a numerical study for the simulation of blood flow and transport processes in large arteries. Blood flow in the arterial lumen was described by incompressible Navier-Stokes equations for Newtonian fluids, while the solute transport was modeled by the diffusion-advection equation. The resistance of the arterial wall to transmural transport is described by a shear-dependent wall permeability model. At the wall-lumen interface, two different transport models for the diffusive flux q_w were assumed. The first model assumed constant wall permeability as follows:

$$q_w = -D \left.\frac{\partial c}{\partial n}\right|_{wall} = \alpha\, c_w \tag{1}$$

where α is a constant wall permeability (Rappitsch and Perktold 1996) and c_w is the wall concentration. In the second model, the permeability of the arterial wall was assumed to be linearly dependent on the local wall-shear stress magnitude $|\tau_w|$:

$$q_w = -D \left.\frac{\partial c}{\partial n}\right|_{wall} = \alpha\, c_w = f\left(|\tau_w|\right) c_w = \beta\, |\tau_w|\, c_w \tag{2}$$

where β is constant.

A more physical boundary condition, which is a function of blood-side solute concentration at the wall and an endothelial permeability parameter, was used by Wada and Karino (1999, 2002) and Ethier (2002) at the blood-wall interface which states that the amount of LDL passing into the vessel wall is determined as the difference between the amount carried to the arterial wall by a filtration flow and the amount which diffuses back to the mainstream. Mathematically, this takes the form:

$$c_w u_w - D \left.\frac{\partial c}{\partial n}\right|_{wall} = \kappa\, c_w \tag{3}$$

where u_w is the filtration velocity at the vessel wall (transmural velocity) which was assumed to be 4×10^{-5} mm/s for a natural artery (Tedgui and Lever 1984, Wilens and McCluskey 1952). The permeability coefficient of LDL (κ) at the arterial wall was about 2×10^{-7} mm/s as reported by Truskey et al. (1992). Qui and Tarbell (2000) analyzed numerically oxygen mass transfer in a compliant curved tube model of a coronary artery using a finite element method. They showed that oxygen can be transported from the lumen to the vessel wall by convective-diffusive mechanism which depends on the fluid phase mass transfer coefficient (h_m) as follows:

$$-D \left.\frac{\partial c}{\partial n}\right|_{wall} = h_m \left(c_b - c_w\right) \Rightarrow h_m = \frac{-D \left.\frac{\partial c}{\partial n}\right|_{wall}}{\left(c_b - c_w\right)} \tag{4}$$

where c_b and c_w are bulk concentration of oxygen in lumen and the wall concentration, respectively.

2.2 Fluid-Wall Model

Fluid-wall model is a single-layer formulation which models the arterial wall as one single layer of porous medium with homogeneous transport properties. As such, it takes into account transport processes within the arterial wall without excessive computational expense (Moore and Ethier 1997, Stangeby and Ethier 2002a,b, Sun et al. 2006). Either (2002), Stangeby and Ethier (2002a,b) developed a mathematical model to study the transport of macromolecules, such as low density lipoproteins (LDLs), across the artery wall and their accumulation in the wall as related to atherosclerosis. Coupled analysis of lumenal blood flow and transmural fluid flow was achieved through the solution of Brinkman's model. The authors assumed that the concentration field of LDL species does not affect the velocity field in the artery and therefore, the Navier–Stokes and continuity equations for the lumen can be written for an incompressible flow of a Newtonian fluid as follows:

$$\nabla \cdot \vec{V} = 0 \tag{5}$$

$$\frac{\partial \vec{V}}{\partial t} + \vec{V} \cdot \nabla \vec{V} = -\frac{1}{\rho}\nabla P + \nu \nabla^2 \vec{V} \tag{6}$$

The velocity field in the porous wall region is computed using Brinkman's model which is a limiting case of the generalized equation in porous media (Vafai and Tien 1980, 1981, Khanafer et al. 2003, Khanafer and Vafai 2006, Khaled and Vafai 2003) and can be expressed as:

$$\frac{\partial \vec{V}}{\partial t} + \vec{V} \cdot \nabla \vec{V} = -\frac{1}{\rho}\nabla P + \nu \nabla^2 \vec{V} - \frac{\nu \vec{V}}{K} \tag{7}$$

where K is the Darcian permeability of the porous medium. Assuming constant diffusivity, the concentration field is computed via the solution of the mass transport equations as:

$$\frac{\partial c}{\partial t} + \vec{V} \cdot \nabla c = D\nabla^2 c + r \tag{8}$$

Where D is the diffusivity of the species of interest in blood, c is the concentration of the species, and r is the reaction term. A suitable boundary condition must be applied at the blood-wall interface. Ethier (2002) assumed that the amount of the species passing into the wall was determined as the difference between the amount carried to the wall by transmural filtration and the amount that diffuses back to the mainstream:

$$c_w u_w - D\frac{\partial c}{\partial n} = \kappa\, c_w \tag{3}$$

Sun et al. (2006) utilized the fluid-wall model to treat the arterial wall as a single-layer of porous medium assuming shear-dependent endothelial transport properties to study the effects of wall shear stress on the transport of LDL and oxygen from blood to and within the wall in an idealized model of a stenosed artery. The transmural flow in the arterial wall was modeled by Darcy's Law:

$$u_w - \nabla \cdot \left(\frac{K}{\mu_p} p_w\right) = 0 \tag{9}$$

Where u_w is the velocity of transmural flow, p_w is the pressure in the arterial wall and μ_p is the viscosity of the blood plasma. Mass transfer in the arterial wall is coupled with the transmural flow and modeled by the convection-diffusion reaction equation as follows:

$$\nabla \cdot (-D_w \nabla c_w + K_{sl} c_w \boldsymbol{u}_w) = k_w c_w \tag{10}$$

Where D_w is the solute diffusivity in the arterial wall, K_{sl} is the solute lag coefficient, and k_w is the consumption rate constant. Transport processes in the arterial wall were coupled with the blood flow in the lumen by Kedem and Katchalsky (1958) equations:

$$J_v = L_p\,(\Delta p - \sigma_d \Delta \pi) \tag{11}$$

$$J_s = P\Delta c + (1 - \sigma_f) J_v \bar{c} \tag{12}$$

Where J_v is the transmural velocity, J_s is the solute flux, L_p is the hydraulic conductivity of the endothelium, Δc is the solute concentration difference across the endothelium, Δp is the pressure across the endothelium, $\Delta \pi$ is the osmotic pressure differential, σ_d and σ_f are the Staverman filtration and osmotic reflection (which accounts for the selective permeability of the biological membranes to certain solutes) coefficients respectively, and $\bar{c}$ is the mean endothelial concentration. Shear-dependent hydraulic conductivity was assumed by Sun et al. (2006) for LDL and oxygen transport, respectively, as follows:

$$L_p\,(|\tau_w|) = 0.392 \times 10^{-12} \ln(|\tau_w| + 0.015) + 2.7931 \times 10^{-12} \tag{13}$$

From the above, it is noted that the fluid–wall model approximates the wall structure by a simple homogeneous layer. It is better than the wall-free model. However, it is still quite inaccurate as it ignores the major wall components which are crucial to atherosclerosis (Stangeby and Ethier 2002a,b).

2.3 Multi-Layers Model

Karner and Perktold (2000) and Karner et al. (2001) developed a mathematical model for the description of the mass transport process in the arterial wall coupled with the mass transport in the arterial lumen. Volume-averaged stationary convection-diffusion equation with a reaction term describing metabolic process was used for the description of the mass transport processes in the intima and media. The filtration velocity in the intima and media was calculated using Darcy's law. Kedem—Katchalsky equations, which describe the convective and diffusive flux across the endothelium and internal elastic lamina (IEL) were utilized to couple the transport equations in the lumen, intima, and media. The physical parameters of the intima and media were obtained from fiber matrix models (Curry 1984, Huang et al. 1992, Huang and Tarbell 1997). Pore theory equations (Curry 1984, Crone and Levitt 1984) were utilized to determine the transport parameters of the endothelium and IEL. The filtration velocity in the wall layer was determined using Darcy's law. The description of the mass transport processes in the intima and media uses the volume-averaged stationary convection-diffusion-reaction equation:

$$\nabla \cdot (-D_w \nabla c_w + K_{sl} c_w \boldsymbol{u}_w) = k_w c_w \tag{10}$$

The transport parameters in the above equation (D_w, K_{sl}, k_w) were calculated using an appropriate fiber matrix model (Curry 1984, Huang and Tarbell 1997, Huang et al. 1992). The transport processes in the lumen, intima and media were coupled by the flux across the endothelium and IEL which was mathematically modeled using the Kedem—Katchalsky equations. The continuity of convective-diffusive flux at the interfaces between lumen, endothelium, intima, IEL, and media was assumed as follows:

$$-D\frac{\partial c}{\partial n} + \mathrm{v}c = J_s = -D_w\frac{\partial c_w}{\partial n} + u_w c_w \tag{14}$$

2.4 Other Models

Several analytical and numerical works have explored the mechanism of transport of macromolecules within the artery wall. Huang and Tarbell (1997) studied the transport and reaction processes for ATP (Adenosine triphasphate) and LDL in the media, which they modeled as a heterogeneous material consisting of a continuous interstitial porous media phase and an array of cylindrical SMCs embedded in the interstitial phase. They did not consider the entrance effects associated with the distribution of material in the media through fenestral pores in the internal elastic lamina (IEL). Tada and Tarbell (2004) developed a two-dimensional numerical model to analyze the effect of the IEL on convective-diffusive transport of macromolecules in the media. The IEL was modeled as an impermeable barrier to both water and solute except for the fenestral pores that were assumed to be uniformly distributed over the IEL. The media was modeled as a heterogeneous medium composed of an array of smooth muscle cells (SMCs) embedded in a continuous porous medium representing the interstitial proteoglycan and collagen fiber matrix (Fig. 1).

The governing equation for the fluid flow in the media is the Brinkman's equation:

$$\nabla P = \mu\nabla^2\boldsymbol{u} - \frac{\mu\boldsymbol{u}}{K_p} \tag{15}$$

and the continuity equation

$$\nabla\cdot\boldsymbol{u} = 0 \tag{16}$$

where K is the Darcian permeability of the extracellular matrix. Solute transport through the extracellular matrix is described by a convective-diffusion equation

$$K_{cf}\boldsymbol{u}\cdot\nabla c = D_f\nabla^2 c \tag{17}$$

where K_{cf} is the lag coefficient for convective transport in the fiber matrix, c is the interstitial macromolecule concentration, and D_f is the effective diffusivity of solutes in the fiber matrix. The boundary condition on the surface of a smooth muscle cell (SMC) is

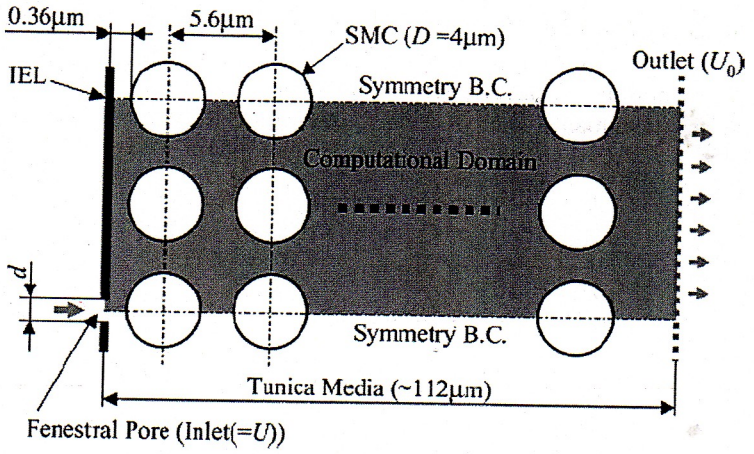

Fig. 1 Schematic illustration of the arterial media underneath the subendothelial layer. Internal elastic lamina (IEL) has a single fenestral pore (Tada and Tarbell 2004)

$$k_r c = D_f \nabla c \tag{18}$$

where k_r is the rate constant associated with the rate of disappearance of solute by surface reaction or cell permeation. In modeling solute uptake by SMCs, Adenosine triphosphate (ATP) and LDL were chosen as substances representing a broad range of molecular size. The degradation of ATP (hydrolysis of ATP to ADP: adenosine diphosphate) on the surface of SMC can be modeled using Michaelis-Menten kinetics with a rate

$$V = \frac{V_{\max} C_s}{k_m + C_s} \tag{19}$$

where $V_{\max}$ is the maximum rate, c_s is the surface concentration, and k_m is the Michaelis constant. For pseudo-first order reaction rate ($c_s << k_m$), the above equation reduces to

$$V = \frac{V_{\max} C_s}{k_m + C_s} \cong \frac{V_{\max}}{k_m} C_s = k_r C_s \tag{20}$$

The effective reaction rate coefficient for ATP was taken as $k_r = 1.25 \times 10^{-4}$ cm/s based on experimental data for $V_{\max}$ and k_m (Gordon et al. 1989) and the effective diffusivity (D_f) was set at $D_f = 2.36 \times 10^{-6}$ cm^2/s (Gordon et al. 1989).

3 Physiological Parameters

The physiological parameters of the various wall layers used in the transport equations were calculated using pore and fiber matrix models, in vivo and in vitro experiments.

3.1 Endothelium and Internal Elastic Lamina

Traditionally, transport characterization across the endothelium and IEL is represented by the Staverman-Kedem–Katchalsky membrane transport equations given as

$$J_v = \frac{K'}{\mu}(\Delta p - \sigma_d \Delta \pi) = L_p(\Delta p - \sigma_d \Delta \pi) \tag{21}$$

$$J_s = D'_e \Delta c + (1 - \sigma_f) J_v \bar{c} = P \Delta c + (1 - \sigma_f) J_v \bar{c} \tag{22}$$

where D'_e is the effective diffusivity per unit length and K' is the permeability per unit length. Using pore theory, some researchers (Prosi et al. 2005, Karner et al. 2001) have derived $L_{p,endothelium} = 3 \times 10^{-9}$ mm^2 s/g, $L_{p,IEL} = 3.05 \times 10^{-7}$ mm^2 s/g, $D'_{e,endothelium} = 3 \times 10^{-10}$ mm/s, and $D'_{IEL} = 1.59 \times 10^{-6}$ mm/s for LDL.

3.2 Intima and Media

The subendothelial intima was modeled as an extracellular matrix of randomly distributed fibers (proteoglycan and collagen). Curry (1984) demonstrated that the partition coefficient ϕ_f (space available to the solute relative to the space available to water) was given by:

$$\phi_f = \exp\left[-(1 - \varepsilon)\left(\frac{2 r_{sol}}{r_f} + \frac{r_{sol}^2}{r_f^2}\right)\right] \tag{23}$$

Where ε is the porosity defined as:

$$\varepsilon = 1 - \pi r_f^2 l_t \tag{24}$$

Where r_f, r_{sol} are the radii of fiber and solute respectively, and l_t is the total length of fibers per unit volume. The Staverman reflection coefficients σ_f and σ_d for the convective transport in the fiber matrix can be expressed as (Curry 1984):

$$\sigma_f = \sigma_d = (1 - \phi_f)^2 \tag{25}$$

The diffusivity coefficient in the intimal extracellular fiber matrix was calculated as follows (Ogston et al. 1973):

$$D_f = D \exp\left[-(1 - \varepsilon)^{0.5}\left(1 + \frac{r_{sol}}{r_f}\right)\right] \tag{26}$$

The Darcy permeability K was given as (Vafai and Tien 1980, 1981, Vafai 1984, Huang et al. 1992):

$$K = \frac{r_f^2 \varepsilon^3}{4G(1-\varepsilon)^2} \tag{27}$$

Where G is the Kozeny constant. Similar to the intima, media was modeled as a medium composed of smooth muscle cells (porosity $= \varepsilon_{SMC}$) and an extracellular fluid phase with fibers (porosity $= \varepsilon$). Therefore, the porosity of the media is given by

$$\varepsilon_m = \varepsilon(1 - \varepsilon_{SMC}) \tag{28}$$

4 Mathematical Model of Macromolecule Transport within the Arterial Wall

Multilayer model is the most complex model which takes into account the heterogeneous properties of the layers constituting the wall. Due to its complexity, a larger number of parameters are required to characterize the physical properties of each layer (Fry 1985, Karner et al. 2001). Most of the previous multilayer models were based on the assumption that the physical properties of the porous wall can be identified by the pore theory. However, this approach does not provide logical estimations. Prosi et al. (2005) proposed a new methodology which starts from a set of data that can be more easily determined by experimental measurements. However, some of the assumptions made in this model give substantial errors. For example, the Kedem–Katchalsky equations used for endothelium and IEL do not take into account the boundary effects associated with the flow across these two layers. In fact, these effects are large due to the thinness of these two layers. Also, they take into account the effects of the reaction inside the media layer by approximating the loss of mass flux upstream of the layer. This simplification can lead to an over or underestimation of the influence of the chemical reaction

Yang and Vafai (2006, 2008), Ai and Vafai (2006), and Khakpour and Vafai (2008a, b) developed a new fundamental four-layer model for the description of the mass transport in the arterial wall coupled with the mass transport in the arterial lumen. The endothelium, intima, internal elastic lamina (IEL) and media layers were all treated as macroscopically homogeneous porous media and mathematically modeled using proper types of the volume averaged porous media equations with the Staverman filtration and osmotic reflection coefficients employed to account for selective permeability of each porous layer to certain solutes. The typical anatomical structure of an arterial wall is shown schematically in Fig. 2.

4.1 Lumen

Blood flow in the arterial lumen was described by the Navier–Stokes and continuity equations assuming incompressible Newtonian fluid as follows:

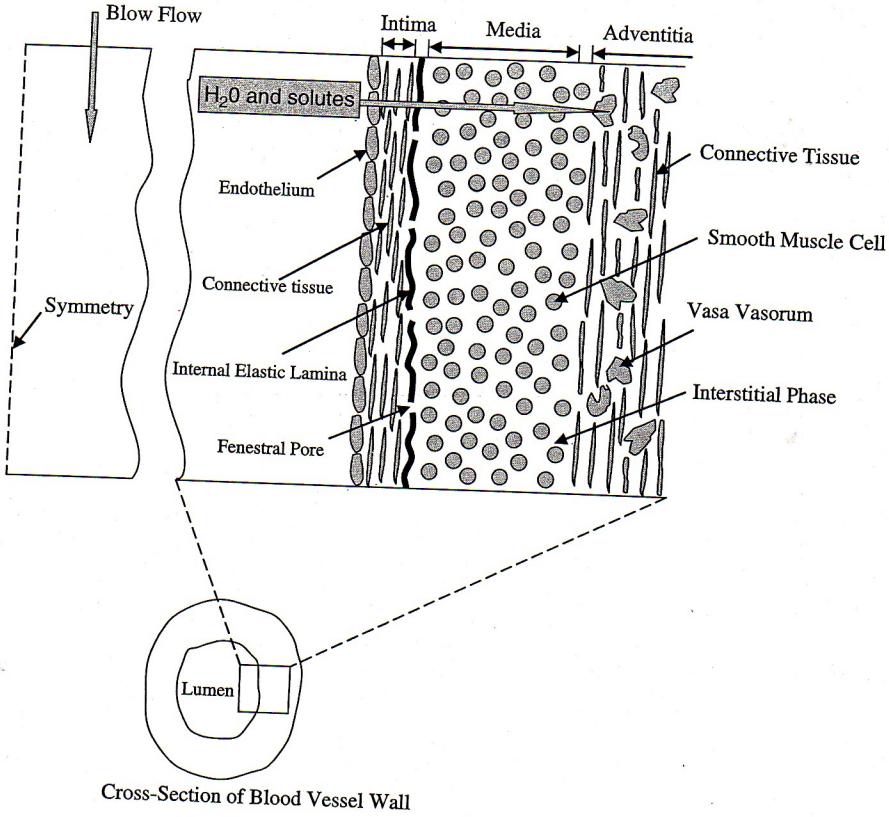

Fig. 2 Schematic illustration of the geometric artery wall

$$\nabla \cdot \vec{V} = 0 \tag{5}$$

$$\frac{\partial \vec{V}}{\partial t} + \vec{V} \cdot \nabla \vec{V} = -\frac{1}{\rho} \nabla P + \nu \nabla^2 \vec{V} \tag{6}$$

The concentration field in the arterial lumen is computed using the mass transport equation:

$$\frac{\partial c}{\partial t} + \vec{V} \cdot \nabla c = D \nabla^2 c \tag{29}$$

4.2 Endothelium and Internal Elastic Lamina

The endothelium and internal elastic lamina (IEL) were modeled as biological porous membranes (Ai and Vafai 2006, Yang and Vafai 2006). The Staverman fil-

tration and osmotic reflection coefficients were employed to account for selective rejection of species by the membranes and for the effects of osmotic pressure. The volume averaged governing equations were given by:

$$\nabla \cdot < \vec{V} > = 0 \tag{30}$$

$$\frac{\rho}{\varepsilon}\frac{\partial < \vec{V} >}{\partial t} = -\nabla < p >^f + \frac{\mu}{\varepsilon}\nabla^2 < \vec{V} > - \frac{\mu < \vec{V} >}{K} + R_u T \sigma_d \nabla < c > \tag{31}$$

$$\frac{\partial < c >}{\partial t} + (1 - \sigma_f) < \vec{V} > \cdot \nabla < c > = D_e \nabla^2 < c > \tag{32}$$

where K is the permeability, and D_e is the effective LDL diffusivity in the medium. The parameters σ_f and σ_d are the Staverman filtration and osmotic reflection coefficients (to account for selective permeability of biological membrane to certain solutes), respectively, T is the absolute temperature of the medium, and R_u is the universal gas constant. The symbol $< >$ denotes the local volume average of a quantity (Vafai and Tien 1980, 1981), and the superscript f refers to the local volume average inside the fluid.

4.3 *Intima and Media*

The intima and media were also modeled as macroscopically homogeneous porous media. Since the porous media are selectively permeable to certain species such as LDL, the Staverman filtration reflection coefficient has to be introduced to account for this effect. The osmotic effect in the transport modeling is not included in this part since the maximum osmotic pressure gradient in the medial layer is far below the hydraulic pressure gradient (Huang and Tarbell 1997). Therefore, the volume averaged governing equations of the intima and media layers are (Alazmi and Vafai 2000, 2001)

$$\nabla \cdot < \vec{V} > = 0 \tag{30}$$

$$\frac{\rho}{\varepsilon}\frac{\partial < \vec{V} >}{\partial t} = -\nabla < p >^f + \frac{\mu}{\varepsilon}\nabla^2 < \vec{V} > - \frac{\mu < \vec{V} >}{K} \tag{31}$$

$$\frac{\partial < c >}{\partial t} + (1 - \sigma_f) < \vec{V} > \cdot \nabla < c > = D_e \nabla^2 < c > + k(c) \tag{32}$$

where k is the effective volumetric first-order reaction rate coefficient. To verify the results obtained using this model, a comparison between the numerical result for species profiles in the media and an exact solution was carried out by Yang and Vafai (2006). This comparison is displayed in Fig. 3. The exact solution was derived based on an assumption that the LDL transport in the media is one-dimensional, with constant filtration velocity. It can be seen from Fig. 3 that the results of porous model results are in excellent agreement with the exact solutions.

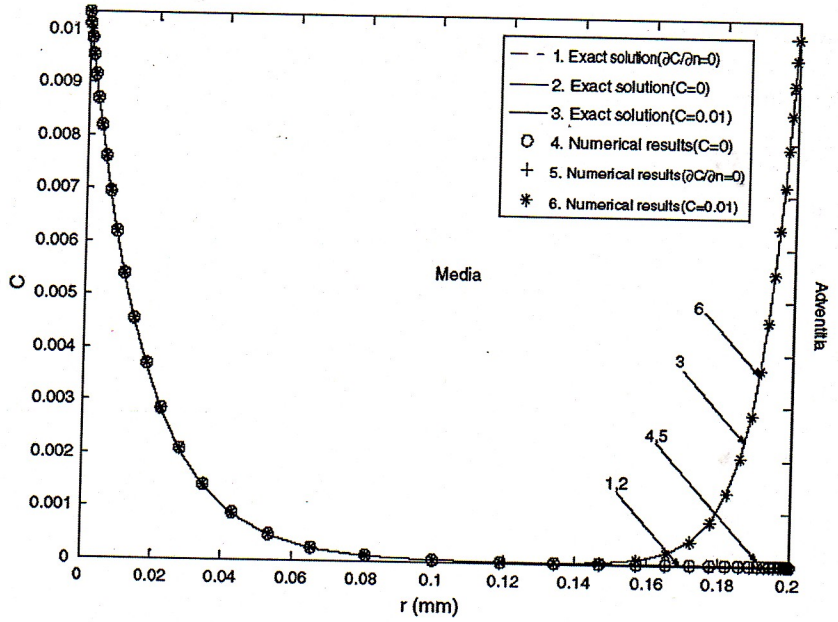

Fig. 3 Comparison between the numerical dimensionless LDL profiles in the media for three different types of concentration boundary conditions at the media adventitia interface and the exact solutions

An additional check on the accuracy of their model, Table 1 illustrates a comparison between the values of the filtration velocity and species concentration taken from literature and the results obtained using porous medium approach. The numerical species concentrations at each interface were found close to the experimental data by Meyer et al. (1996) and numerical results by Prosi et al. (2005).

Tables 2 and 3 show a summary of different boundary conditions used at the interface between the lumen and the arterial wall as well as various momentum equations used in modeling the flow in the arterial wall.

Table 1 Comparison between the values of the filtration velocity and species concentration taken from literature and the porous model (Nang and Vafai , 2006)

	Meyer et al. (1996)	Prosi et al. (2005) $C = 0$	Porous Model $C = 0$
Filtration velocity (mm/s)	1.78×10^{-5}	1.76×10^{-5}	2.31×10^{-2}
Species Concentration			
Lumen-endothelium interface	1.026	1.0262	1.0246
Intima-IEL interface	N/A	2.716×10^{-2}	3.983×10^{-2}
IEL-media interface	1.00×10^{-2}	8.58×10^{-3}	1.033×10^{-2}
Media (r = 3.214 mm)	2.5×10^{-3}	2.23×10^{-3}	2.687×10^{-5}
Media-adventitia interface	1.00×10^{-2}	0.00	0.00

Table 2 Summary of the mass interface boundary conditions between lumen and arterial wall

Model	Remarks
$-D\left.\frac{\partial c}{\partial n}\right\|_{wall} = \alpha\, c_w$	-wall free model -constant wall permeability
$-D\left.\frac{\partial c}{\partial n}\right\|_{wall} = \alpha\, c_w = f(\lvert\tau_w\rvert)\, c_w = \beta\, \lvert\tau_w\rvert\, c_w$	-wall free model -permeability is linearly dependent on the local shear stress magnitude
$c_w u_w - D\left.\frac{\partial c}{\partial n}\right\|_{wall} = \kappa\, c_w$	-wall free model and fluid-wall model -more realistic -depends on the blood-side solute concentration at the wall, endothelial permeability parameter, and the filtration velocity
$-D\left.\frac{\partial c}{\partial n}\right\|_{wall} = h_m\,(c_b - c_w)$	-wall free model -depends on the bulk concentration in the lumen and the arterial wall concentration

*w: interface between the lumen and the arterial wall

Table 3 Summary of the momentum equation used in the arterial wall

Model	Remarks
$u_w - \nabla \cdot \left(\frac{K}{\mu_p} p_w\right) = 0$	-fluid-wall model -arterial wall modeled as single-layer porous medium -Darcy model -constant permeability
$\frac{\partial \vec{V}}{\partial t} + \vec{V} \cdot \nabla \vec{V} = -\frac{1}{\rho}\nabla P + \nu \nabla^2 \vec{V} - \frac{\nu \vec{V}}{K}$	-fluid-wall model -arterial wall modeled as single-layer porous medium -Brinkman's model -constant permeability
$\frac{\rho}{\varepsilon}\frac{\partial <\vec{V}>}{\partial t} = -\nabla < p >^f + \frac{\mu}{\varepsilon}\nabla^2 < \vec{V} > - \frac{\mu <\vec{V}>}{K} + R_u T \sigma_d \nabla < c >$	-endothelium and internal elastic lamina -more realistic -The Staverman filtration and osmotic reflection coefficients were employed to account for selective rejection of species by the membranes and for the effects of osmotic pressure
$\frac{\rho}{\varepsilon}\frac{\partial <\vec{V}>}{\partial t} = -\nabla < p >^f + \frac{\mu}{\varepsilon}\nabla^2 < \vec{V} > - \frac{\mu <\vec{V}>}{K}$	-intima and media -more realistic -accounts for Staverman filtration reflection coefficient -neglects the osmotic effect in the transport modeling

5 Future Directions

In the cardiovascular system, blood flow is under constant interaction with arterial walls. The interactions between blood flow and wall deformation can involve a wide range of fluid- mechanical phenomena. When blood flows through the lumen, the forces associated with the flow may deform the arterial walls and consequently alter the properties of the wall which in turn affect the flow structure in the lumen as well as the transport process of macromolecules from the lumen to the arterial walls. This will have an impact on the development of many diseases such as atherosclerosis. Most previous studies have been carried out under different simplifying assumptions such as steady flow, rigid boundary, Newtonian fluid, etc. The comparison between the simulations considering rigid arteries and deformable arteries have shown a substantial increase in the wall shear stresses for a rigid artery. This indicates that as the artery becomes more rigid, its wall shear stress increases leading to atherosclerosis. Hence, simultaneous fluid-structure interactions (FSIs) should be considered when studying the hemodynamics, flow structure, and the transport of macromolecules from the lumen to the arterial walls. Transient FSI simulations may provide physical insight to the mechanisms of the atherosclerosis. The solution of fluid-structure interaction problems, coupling computational fluid dynamics analysis with finite element stress analysis, is now becoming tractable through the accessibility of high performance computing.

There is a need for an FSI approach in studying the transport of macromolecules in the arterial walls under pulsatile flow condition and utilizing a porous media approach to analyze the arterial walls. Since the wall of the artery is deformable, a complex coupling exists between the flow in the lumen and the arterial wall. Thus, the variations in the porosity and permeability of the deformable arterial wall should be considered in such analysis. In addition, the variations in the physical properties of the arterial walls such as Young modulus and Poisson's ratio should be considered in any future studies since the materials of the walls are nonlinear, non-homogeneous, and anisotropic.

Nomenclature

D diffusion coefficient
D'_e effective diffusivity per unit length
c concentration
c_b bulk concentration
c_s surface concentration
c_w wall concentration (at the interface between lumen and the arterial wall)
$\bar{c}$ mean endothelial concentration
h_m fluid phase mass transfer coefficient
J_s solute flux

k_m Michaelis constant
k_w consumption rate constant
K Darcian permeability
K_{sl} solute lag coefficient
L_p hydraulic conductivity of the endothelium
p_w pressure in the arterial wall
q_w diffusive wall flux
r reaction term
u_w transmural velocity
$V_{\max}$ maximum rate

Greek Symbols

α constant wall permeability
β proportionality factor (shear-dependent wall permeability model)
$\Delta\pi$ osmotic pressure differential
κ The permeability coefficient at the arterial wall
μ_p viscosity of the blood plasma
ε porosity
σ_d Staverman filtration
σ_f osmotic reflection

References

Ai L, Vafai K (2006) A coupling model for macromolecule transport in a stenosed arterial wall, Int. J. Heat Mass Transf. 49: 1568–1591.
Alazmi B, Vafai K (2001) Analysis of fluid flow and heat transfer interfacial conditions between a porous medium and a fluid layer. Int. J. Heat Mass Transf. 44: 1735–1749.
Alazmi B, Vafai K (2000) Analysis of variants within the porous media transport models. ASME J. Heat Transfer 122: 303–326.
Back L, Radbill J, Crawford D (1977) Analysis of oxygen transport from pulsatile, viscous blood flow to diseased coronary artery of man. J. Biomech. 10: 763–774.
Crone C, Levitt DG (1984) Capillary permeability to small solutes. In: Handbook of Physiology. Microcirculation. The Cardiovascular System, Section 2, Vol. IV, Pt. 1, American Physiological Society, Bethesda, MD, pp. 411–466 (Chapter 8).
Curry FE (1984) Mechanics and thermodynamics of transcapillary exchange. In: Handbook of Physiology. Microcirculation. The Cardiovascular System, Section. 2, Vol. IV, Pt. 1, American Physiological Society, Bethesda, MD, pp. 309–374 (Chapter 8).
Ehrlich L, Friedman M (1977) Steady convective diffusion in a bifurcation. IEEE Trans. Biomed. Eng. 24: 12–18.
Ethier CR (2002) Computational modeling of mass transfer and links to atherosclerosis, Ann. Biomed. Eng. 30: 461–471.
Fry DL (1985) Mathematical models of arterial transmural transport. Am. J. Physiol. 248: H240–H263.

Fry DL (1987), Mass transport, atherogenesis and risk, Arteriosclerosis 7: 88–100.
Gordon EL, Pearson JD, Dickinson ES, Moreau E, Slakey L (1989) The hydrolysis of extraceller adenine nucleotides by arterial smooth muscle cells. J. Biol. Chem. 15: 18986–18992.
Hoff HF, Heideman CL, Jackson RL, Bayardo RJ, Kim HS, and Gotto AMJ (1975) Localization patterns of plasma apolipoproteins in human atherosclerotic lesions. Circ. Res. 37: 72–79.
Huang ZJ, Tarbell JM (1997) Numerical simulation of mass transfer in porous media of blood vessel walls, Am. J. Physiol. 273: H464–H477.
Huang Y, Rumschitzki D, Chien S, Weinbaum S (1994) A fiber matrix model for the growth of macromolecular leakage spots in the arterial intima, J. Biomech. Eng. 116: 430–445.
Huang Y, Weinbaum S, Rumschitzki D, Chien S (1992) A fiber matrix model for the growth of macromolecular leakage spots in the arterial intima. In: Advances in Biological Heat and Mass Transfer, HTD-Vol. 231. ASME, New York, pp. 81–92.
Karner G, Perktold K (2000) Effect of endothelial injury and increased blood pressure on albumin accumulation in the arterial wall: a numerical study. J. Biomech. 33: 709–715.
Karner G, Perktold K, Zehentner HP (2001) Computational modeling of macromolecule transport in the arterial wall, Comput. Meth. Biomech. Biomed. Eng. 4: 491–504.
Kedem O, Katchalsky A (1958) Thermodynamic analysis of the permeaility of biological membranes to non-electrolytes. Biochem. Biophys. Acta. 27: 229–246.
Khakpour M, Vafai K (2008a) A critical assessment of arterial transport models. Int. J. Heat Mass Transfer 51: 807–822.
Khakpour M, Vafai K (2008b) A compelete analytical solution for mass transport within a multilayer arterial wall. In press for Int. J. Heat Mass Transfer.
Khaled A-RA, Vafai K (2003) The role of porous media in modeling flow and heat transfer in biological tissues. Int. J. Heat Mass Transfer 46: 4989–5003.
Khanafer K, Vafai K (2006) The role of porous media in biomedical engineering as related to magnetic resonance imaging and drug delivery, Heat Mass Trans. 42: 939–953.
Khanafer K, Vafai K, Kangarlu A (2003) Computational modeling of cerebral diffusion-application to stroke imaging. Magn. Reson. Imag. 21: 651–661.
Meyer G, Merval R, Tedgui A (1996) Effects of pressure-induced stretch and convection on low-density lipoprotein and albumin uptake in the rabbit aortic wall, Circ. Res. 79: 532–540.
Moore JA, Ethier CR (1997) Oxygen mass transfer calculations in large arteries. ASME J. Biomech. Eng. 119: 469–475.
Newby AC, Zaltsman AB (2000) Molecular mechanisms in intimal hyperplasia. J. Pathol. 190: 300–309.
Ogston AG, Preston BN, and Wells JD (1973) On the transport of compact particles through solutions of chain polymer, Proc. R. Soc. London Ser. A 333: 297–316.
Prosi M, Zunino P, Perktold K, and Quarteroni A (2005) Mathematical and numerical models for transfer of low-density lipoproteins through the arterial walls: a new methodology for the model set up with applications to the study of disturbed luminal flow. J. Biomech. 38: 903–917.
Qui YC, Tarbell JM (2000) Numerical simulation of oxygen mass transfer in a compliant curved tube model of a coronary artery, Ann. Biomed. Eng. 28: 26–38.
Rappitsch G, Perktold K (1996) Pulsatile albumin transport in large arteries: a numerical simulation study. ASME J. Biomech. Eng. 118: 511–519.
Rappitsch G, Perktold K, Pernkopf E (1997) Numerical modeling of shear dependent mass transfer in large arteries. Int. J. Numer. Methods Fluids 25: 847–857.
Ross R(1993) Atherosclerosis: a defense mechanism gone awry. Am. J. Pathol. 143: 987–1002.
Schwenke DC, St. Clair RW (1993) Influx, efflux, and accumulation of LDL in normal arterial areas and atherosclerotic lesions of white Carneau pigeons with naturally occurring and cholesterol-aggravated aortic atherosclerosis. Arterioscler. Thromb. Vasc. Biol. 13: 1368–1381.
Stangeby DK, Ethier CR (2002a) Coupled computational analysis of arterial LDL transport-effects of hypertension, Comput. Meth. Biomech. Biomed. Eng. 5: 233–241.
Stangeby DK, Ethier CR (2002b) Computational analysis of coupled blood-wall arterial LDL transport, J. Biomech. Eng. 124: 1–8.

Sun N, Wood NB, Hughes AD, Thom AS, Xu XY (2006) Fluid-Wall modelling of mass transfer in an axisymmetric stenosis. Ann. Biomed. Eng. 34: 1119–1128.
Tada S, Tarbell JM (2004) Internal elastic lamina affects the distribution of macromolecules in the arterial wall: a computational study, Am. J. Physiol. 287: H905–H913.
Tedgui A, Lever MJ (1984) Filtration through damaged and undamaged rabbit thoracic aorta. Am. J. Physiol. 247: H784–H791.
Truskey GA, Roberts WL, Herrmann RA, Malinauskas RA (1992) Measurement of endothelial permeability to 125I-low density lipoproteins in rabbit arteries by use of enface preparations. Circ. Res. 71: 883–897.
Vafai K (1984) Convective flow and heat transfer in variable porosity media J. Fluid Mech. 147: 233–259.
Vafai K, Tien CL (1980) Boundary and inertia effects on flow and heat transfer in porous media. Int. J. Heat Mass Transf. 24: 195–203.
Vafai K, Tien C L (1981) Boundary and inertia effects on convective mass transfer in porous media. Int. J. Heat Mass Transf. 25: 1183–1190.
Wada S, Karino T (1999) Theoretical study on flow-dependent concentration polarization of low density lipoproteins at the luminal surface of a straight artery, Biorheology 36: 207–223.
Wada S, Karino T (2000) Computational studyon LDL transfer from flowing blood to arterial walls. In: Yamaguchi, T. (Ed.), Clinical Application of Computational Mechanics to the Cardiovascular System. Springer, Berlin, 157–173.
Wada S, Karino T (2002) Theoretical prediction of low-density lipoproteins concentration at the luminal surface of an artery with a multiple bend, Ann. Biomed. Eng. 30: 778–791.
Wilens SL, McCluskey RT (1952) The comparative filtration properties of excised arteries and veins. Am. J. Med. 224: 540–547.
Yuan F, Chien S, Weinbaum S (1991) A new view of convective–diffusive transport processes in the arterial intima, J. Biomech. Eng. 133: 314–329.
Yang N, Vafai K (2006) Modeling of low-density lipoprotein (LDL) transport in the artery—effects of hypertension, Int. J. Heat Mass Transf. 49: 850–867.
Yang N, Vafai K (2008) Low density lipoprotein (LDL) transport in an artery-A simplified analytical solution. Int. J. Heat Mass Transfer 51: 497–505.